Manuscript submitted to: Volume 1, Issue 3, 132-142.

*AIMS Materials Science* DOI: 10.3934/matersci.2014.3.132

Received date 31 March 2014, Accepted date 16 June 2014, Published date 1 July 2014

*Research Article*

# Microstructural characterization of laser sintered synthetic calcium phosphate-natural dentine interface for the restoration of enamel surface

**Animesh Jha [1,*], Esam Elmadani [1], Tejaswini Peralli [1], Monty S Duggal [2], David Walsh [3], Christine Jappy [3], Tom Brown [3] and Wilson Sibbett [3]**

[1] The Institute for Materials Research, Houldsworth Building, University of Leeds Leeds LS2 9JT, UK

[2] Leeds Dental School, Worsley Building, University of Leeds, Leeds LS2 9JT

[3] School of Physics and Astronomy, University of St Andrews, St Andrews KY16 9SS, UK

*** Correspondence:** Email: a.jha@leeds.ac.uk;

**Abstract:** Tooth sensitivity is a common occurrence and it is caused by acid induced erosion of enamel surface. In this investigation we report the results of calcium phosphate based minerals which are irradiated with lasers ex vivo for the analysis of photo activated densification of minerals. The photo-activation in these minerals may primarily arise from the absorption centres, namely $OH^-$ and rare-earth $(RE)^{3+}$ ion dopants (e.g. $Er^{3+}$ ions) incorporated during synthesis. The loss of hydroxyl group from mineral is characterized using the thermogravimetric technique. The microstructural changes under the conditions of continuous wave (CW) and pulsed laser irradiation are reported together with the measured temperature rise. The preliminary data on surface hardness of occluded dentine with photo-activated calcium phosphate minerals are also reported, for aiming an eventual hardness value of 3300 MPa which is known for natural enamels.

**Keywords:** Calcium phosphate minerals; dental enamel and acid erosion; laser surface modification

## 1. Introduction

Tooth sensitivity is a lifestyle related condition, resulting from the exposure of dentine surface [1,2] and eventually of dentinal tubules to the external stimuli in the oral environment. The movement of the dentinal fluid stimulates the nerves and causes pain [1-3]. Treatments for teeth sensitivity such as nerve desensitization using potassium nitrate [3], and dentinal tubule occlusion using commercial brands of toothpastes such those containing hydroxyapatite (HAp) [4] have shown to be effective only in the short term, as the recurrence of sensitivity is commonly reported [5]. Occlusion of dentinal tubules using HAp nano particles in vitro [6] and in situ via toothpaste [4] has been reported to provide surface protection up to 90% of tubules, which might contribute to the re-mineralization at the root of dentinal tubules [4,7]. HAp is a calcium phosphate (CaP) based apatite with a general chemical formula $M_{10}(XO_4)_6Y_2$ [8,9]. In such phosphate minerals, $M^{2+}$, $(XO_4)^{3-}$,

and/or Y- ions may be substituted, by ions with comparable ionic and molecular radii. For example, $Ca^{2+}$ may be substituted by $Al^{3+}/RE^{3+}$, $(PO4)^{3-}$ ions by $(SiO_4)^{4-}$ and bicarbonate and carbonate, and $OH^-$ by $F^-$, respectively [9,10,11] for various potential hard tissue applications. The incorporation of $RE^{3+}$, $Al^{3+}$ and $F^-$ ions could be very beneficial in producing an acid resistant calcium phosphate composite due to their anti-dental demineralization effect [12]. For analyzing the structure of cations in calcium phosphate minerals, the diffusion of $RE^{3+}$ ions into the phosphate structure was reported to occur only under heating [13].

Historically the neodymium:yttrium-aluminum-garnet (Nd: YAG) and carbon dioxide ($CO_2$) lasers have been widely investigated for the treatment of sensitive teeth by melting dentine surface to seal dentinal tubules [3,14], however, heat accumulation during laser irradiation appears to be the cause of structural changes and damage to dentinal tissues such as phase changes and surface cracks, respectively [15]. Furthermore, under laser irradiation, the $RE^{3+}$ ions have the ability to absorb the energy of photons and emit photons at longer wavelengths and as heat through phonon vibrations [16]. It is unknown at present in the context of dental mineral modification whether any benefit might be reaped by utilizing heat and photons from RE-ion de-excitation.

In the present investigation the use of a photosensitive calcium phosphate mineral is investigated for the analysis of large surface area for occlusion of exposed dentinal tubules. In a related investigation, we reported the method of mineral synthesis and characterization for achieving rare-earth ($RE^{3+}$, e.g. $Er^{3+}$), $Al^{3+}$ and $F^-$ ions in calcium phosphate (brushite, $CaH(PO_4).2(H_2O)$ and monetite, $CaHPO_4$) mineral phase mixture [17]. The $F^-$ ion doping imparts acid-resistance by replacing the OH- ions in the structure [11]. We also focused on forming a calcium phosphate phase mixture which is more stable below pH = 6, under which condition, the hydroxyl apatite (HAp) is a chemically unstable mineral [18]. Finally, unlike monetite and brushite, the needle-shape HAp offers only limited the surface occlusion, as it relies on the morphology of the aggregated minerals for blocking the dentine tubules [6]. By reviewing literature there appears to be no report on any microstructural comparison of laser irradiation induced physical changes.

## 2. Materials and Method

### *2.1. Powder Synthesis*

The synthesis of mineral powder was carried out at room temperature using 0.1 molar concentrations of calcium nitrate tetra-hydrate $Ca(NO_3)_2.4H_2O$ and di-ammonium hydrogen phosphate $(NH_4)_2HPO_4$ (Fisher scientific) in distilled water in 160 mL volume. These two solutions were mixed by stirring while adding di-ammonium hydrogen phosphate solution drop-by-drop into the calcium nitrate tetra-hydrate solution to yield a calcium phosphate suspension with a molar ratio of Ca: P which was maintained in the range of 1 to 1.67. In one batch of synthesis, only calcium phosphate suspension was formed. However, by incorporating analytical grades (Fisher Scientific) of powders of rare-earth erbium oxide ($Er_2O_3$), aluminium phosphate ($AlPO_4$) and calcium fluoride ($CaF_2$) into the stock solution of $(NH_4)_2HPO_4$ and $Ca(NO_3)_2.4H_2O$ solution, the doped calcium phosphate mineral was synthesized. The concentration of each dopant in the stock solution was equivalent to 5 mole percent. After incorporating these crystalline materials, the resulting slurry was then stirred for 1 hour at a speed of ~ 400 rpm, producing a milky mixture, which was then left to standby at room temperature for 24 hours. During this period the solution was covered with a polyethylene film (cling wrap) for minimizing the absorption of atmospheric $CO_2$. Finally, the wet precipitate was collected and dried in an oven at 80 ºC for up to 36 hours in air. The synthesized materials were analyzed for phase and morphological analyses.

*2.2. In Vitro Sample Preparation*

Cross-section of cleaned bovine incisors and extracted and γ-ray irradiated human molars with ~1-2 mm in thickness were prepared by carefully grinding and polishing. These tissue samples were obtained from the Leeds Dental Institute. The sections were then etched with 35% w/v phosphoric acid solution in a stirred bath to remove the natural smear layer and smear plugs. Figure 1a shows the high magnification SEM image showing the micro-meter scale capillaries, called the dentinal tubules. The polished dentine tubule sections were dehydrated using alcohol/water mixtures containing 50%, 70%, 90% and 100% absolute ethanol for 30 minutes in each mixture, in order to minimize the shrinkage of tissue via evaporation of alcohol and water. The cross-sections of human molar tissue were finally left for drying for 24 hours. The dip and extraction method of coating [17] was found to produce a non-uniform coating thickness, and as a result it was necessary to fine grind 5 wt% of synthetic calcium phosphate mineral into a 50 mL ethanol to make thicker coating material having consistency of a toothpaste gel which was then applied over sectioned molars using a very fine paint brush. The manually coated human molars were left for drying via natural evaporation of ethanol, before laser irradiation. In this investigation, for comparative studies, the pressed pellets of calcium phosphate mineral were also examined for the densification mechanism in the pulsed and CW laser sintered minerals.

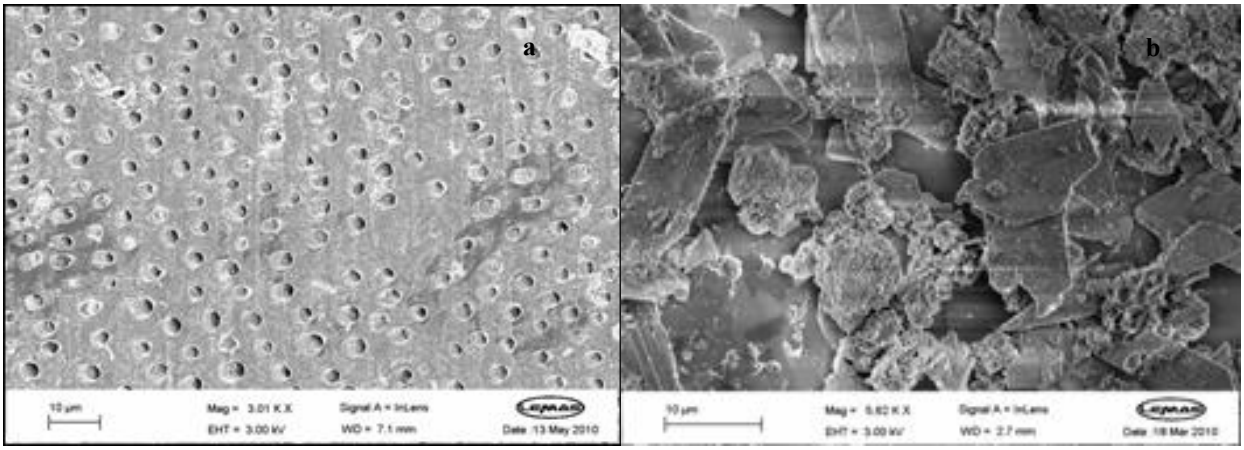


**Figure 1. a) An SEM image of as prepared tooth section, showing the open dentine micro channels that mimic the natural dentine hypersensitivity. b) is an SEM image of platelet-like particles of calcium phosphate minerals, chemically precipitated at room temperature.**

*2.3. Laser Irradiation experiments*

Laser irradiation experiments were carried out in two wavelength bands at 980 nm and 1520 nm, both of which overlap with the corresponding ground state absorptions ($^4I_{15/2} \rightarrow {}^4I_{11/2}$ and $^4I_{15/2} \rightarrow {}^4I_{13/2}$) of $Er^{3+}$ ions [19,20], chosen as the photo-active component of in the mineral phase. The chosen laser sources were: a 980 nm laser continuous wave (CW), a 1520 nm CW laser , and a 1520 nm was a 120 fs pulsed source. The fs-pulsed source was with the output power of 130 mW and a repetition rate of 2.5 GHz, implying that the 2.5 billion pulses per second were incident at the focal spot and each of these pulses interacted with mineral for 120 fs, leading to mineral phase modification. By comparison, the output powers of the 980 nm and 1520 nm CW lasers were at 150 mW. Since the

ground state absorption at 1520 nm (from overall ground state $^4I_{15/2} \rightarrow {}^4I_{13/2}$ optical transition) is much smaller than at $^4I_{15/2} \rightarrow {}^4I_{11/2}$ [20], the $Er_2O_3$ doped minerals and glass absorb much smaller fraction of CW laser energy at 1520 nm than that at 980 nm. This is because of a resonant condition at $^4I_{15/2} \rightarrow {}^4I_{11/2}$. By comparison, in a 1520 nm fs pulsed laser, the average power was 130 mW. Synthetic minerals coated hard enamel surfaces and pressed mineral pellets were irradiated between 30 seconds to 300 seconds in this investigation. For temperature measurements during laser irradiation, a chromel-alumel thermocouple was attached on to the back face of coated and uncoated molar cross-sections for recording the temperature. We point out that in our investigation as the laser stage was not equipped with the motion controller for rastering the entire molar surface for irradiation induced phase change and densification, the power delivery was always referred to a fixed spot size of 250 μm in diameter for which the pictorial examples are shown below.

After laser irradiation, selected human molars were tested for hardness measurements using the Vickers Hardness technique, and the preliminary data on surface hardness of exposed dentine and molar with synthetic enamel mineral are compared below.

## 3. Results and discussion

The laser irradiated cross-sections of human molars and incisors and calcium phosphate pellets were characterized using a FEGSEM electron microscope with an energy dispersive X-ray analyzer. The technique allowed us to compare the effects of the physical changes on phosphate particles and the occlusion of dentinal tubules. Since the residual absorption at 1520 nm wavelength is much less than that at 980 nm, we focus on recording temperature changes only using a 980 nm CW laser.

**Table 1. Temperature change ΔT ($^o$C) measured during 980 nm CW laser irradiation on uncoated and coated molar sections. Total laser irradiation time was 5 minutes. Section thickness= ~1mm.**

| sample | Temperature change (ΔT, $^o$C) measured during CW laser treatments. Error ± 0.5 $^o$C | | |
|---|---|---|---|
| | Initial Temperature, $T_1$, $^o$C | Final temperature $T_2$, $^o$C | ΔT ($T_1$−$T_2$), $^o$C |
| Tooth section | 22.8 | 26 | 3.2 |
| Tooth section coated with calcium phosphate without $Er^{3+}$ ions | 22.8 | 24.9 | 2.1 |
| Tooth section coated with calcium phosphate with $Er^{3+}$ ions | 22.8 | 23.2 | 0.4 |

As shown in Figure 1b, the synthesized mineral particulates have platelet morphology, with an average of 10−15 μm in two large dimensions. The thickness was estimated to be sub micrometer. The X-ray powder diffraction data (Cu $K_\alpha$ radiation) for the minerals with and without dopants are compared in Figure 2, in which the dominant phases are burshite ($CaHPO_4.2H_2O$) and monetite ($CaHPO_4$), with less than 5 phase volume percent of hydroxyl apatite mineral. The details of crystal structure analysis are reported elsewhere [17]. From Figure 2, it is evident that the presence of

dopants in mineral enhances the background due to the presence of amorphous phase. It is likely that the intensity background might have been enhanced due to the presence of $Er^{3+}$-ions in the mineral phase, which has a more complex electronic structure than the lighter elements in the mineral.

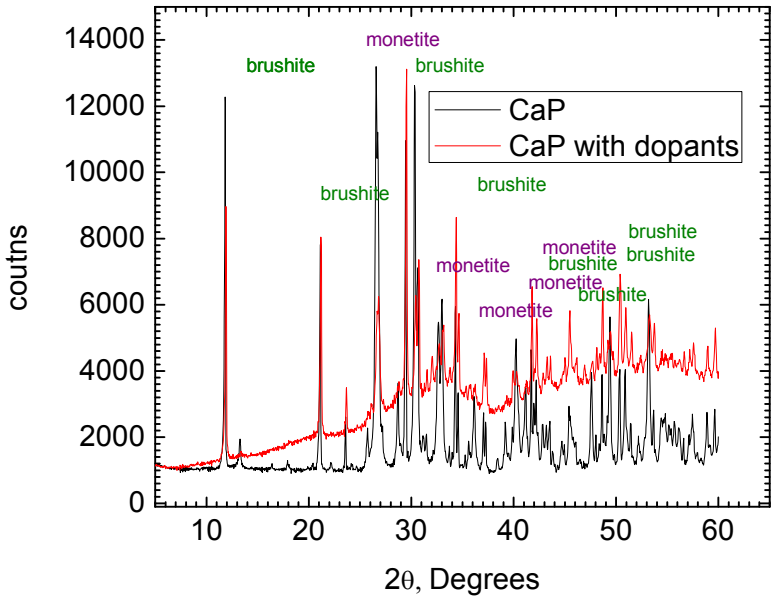


**Figure 2. A comparison of X-ray powder diffraction data for undoped (black colour) and doped calcium phosphate minerals (red colour). Monochromatic X-ray radiation used was a Cu-$K_\alpha$ source.**

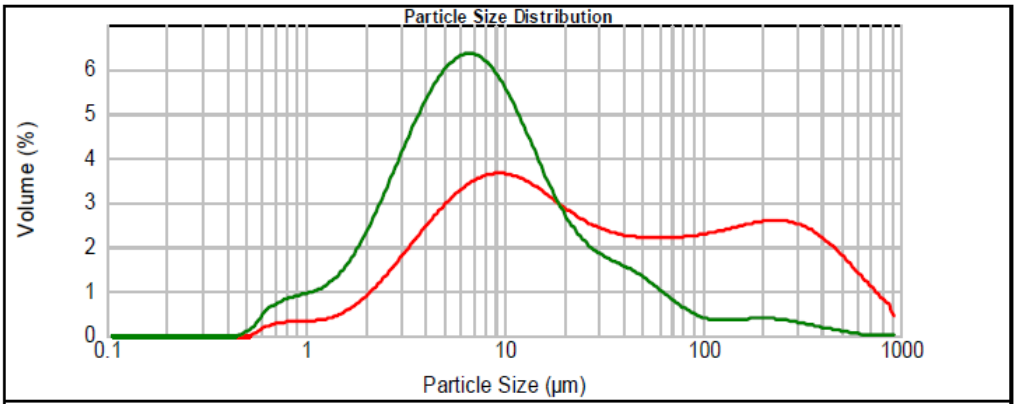


**Figure 3. Particle and particle size distribution analysis of doped (red) and undoped (green) calcium phosphate powders, using a Malvern particle size analyser. The undoped CaP particles have central size distribution below 10 µm, with two satellite peak below sub-micrometer and above 100 µm ranges, respectively. The particle size distribution for doped CaP is bi-modal, with peaks centred at around 10 µm and above 200 µm.**

In Figure 3, the particle size distributions of synthetic doped (red) and undoped (green) minerals are compared, from which it is apparent that the undoped mineral largely appears single modal, with

three satellite distribution peaks below 1 μm (16 vol%) and 30 μm (25 vol%) and 200 μm (<10 vol%), and the remaining volume percent belonging to the main peak centred between 6 and 7 μm. By comparison, the particle size distribution in doped CaP (red curve) in Figure 3 is predominantly bi-modal, with peaks centred around 10 μm and 200 μm. In this case, the sub-micrometer volume percent, relative to the bi-modal distribution, appears comparatively less (<5 vol%) than the undoped mineral size distribution curve. Comparing the particle size distribution data with the SEM microscopic data in Figure 1b, we find a satisfactory morphological comparison, showing that the particulate surface area varies from 5 $\mu m^2$ to 150 $\mu m^2$. Besides these crystalline phase mixture, the unreacted $CaF_2$, $AlPO_4$ and rare-earth oxides were also homogeneously distributed and were present in less than 10–15 volume percent. The platelet-like morphology of calcium phosphate minerals appear to be beneficial, not only in the occlusion of dentinal tubules but also in enhancing the heat transfer during laser irradiation. This morphology is desirable for reducing the risk of soft tissue damage in the dentine tubule structure.

In Figure 4, the percentage weight loss under isochronal heating condition is shown for a pellet formed from doped calcium phosphate powder. It is apparent from this Figure that when mineral is heated it loses more than 50% of its weight by 300 $^oC$, and almost 95% of weight loss occurs by 400 $^oC$. Above 400 $^oC$ until 1000 $^oC$, the remaining weight loss occurs. This weight loss data might help in the analysis of structural changes in minerals, as a result of laser irradiation which is absorbed by the mineral and partly turns into heat.

The effects of irradiation of CW lasers at 1520 nm on undoped CaP mineral surface were first carried out onto pressed pellets of ~1mm in thickness for 1 minute, after which each exposed area was examined under SEM for morphological changes, as shown in Figures 5a and 5b. The examination of surfaces in undoped and $Er_2O_3$-doped CaP surfaces for longer than 1 minute (not included here) of CW irradiation using the 980 nm and 1520 nm lasers reveal that there was little evidence of any apparent melting. However, when the mineral doped with $Er_2O_3$ only and that doped with $Er_2O_3$, $AlPO_4$, and $CaF_2$ was coated over exposed dentine and irradiated for 5 minutes using a 980 nm CW laser, it was apparent that the 980 nm CW laser was promoting more superficial melting than that using a 1520 nm laser.

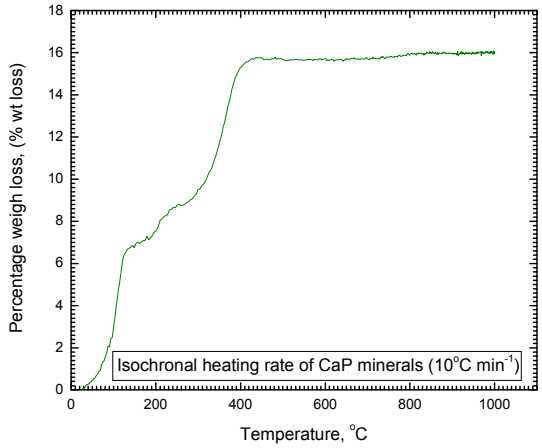


**Figure 4. An isochronal heating rate (10 $^oC$ $min^{-1}$) weight loss curve for undoped calcium phosphate mineral.**

The resulting liquid formed and spread slowly over the surface of exposed dentine. The

spreading behaviour of melted liquid on laser irradiation was more apparent when mineral phase was mixed with $CaF_2$, as compared in Figures 5c and 5d. In Figure 5c discontinuous melting is evident in $Er_2O_3$ doped calcium phosphate, whereas the presence of $CaF_2$, $AlPO_4$, and $Er_2O_3$ in CaP resulted into more continuous regions of melting which solidified with ridge-like feature and rosette-like crystals in Figure 5d. It may be concluded that after 5 minutes of laser irradiation of minerals incorporated with $CaF_2$, $AlPO_4$ and $Er_2O_3$ yielded more uniform melting and spreading than that without $CaF_2$.

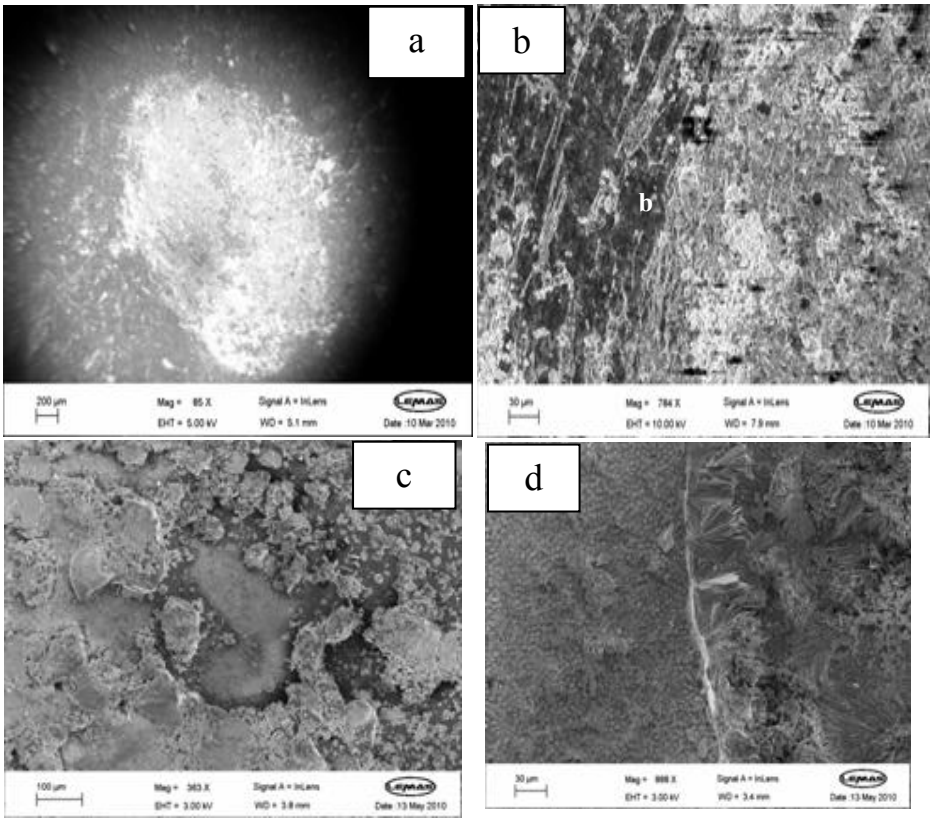


**Figure 5. SEM images of (a–b) CaP- $Er_2O_3$ pellet when irradiated with 1520 nm CW laser and (c) $Er_2O_3$ doped CaP coating and, d) CaP-$Er_2O_3$-$AlPO_4$-$CaF_2$ coating over dentine, each of which was irradiated with a 980 nm CW laser for 5 minutes showing the evidence for localized and extensive melting, respectively. Incident laser power was 150 mW at a focus spot.**

Since the melting induced surface modification using 980 nm CW laser requires at least 5 minutes over 100–250 $\mu m^2$ area, it was decided that for clinical application such an approach might prove too slow for ultimate treatment. It was therefore necessary also to compare the response of these minerals when irradiated with an ultra-fast laser (120 fs, 130 mW). Since a femto-second laser at 980 nm is currently not available, we investigated the structural changes using a fs-1520 nm laser only. Figure 6a is the surface of dentine which was coated with doped CaP mineral. In Figures 6b, 6c and 6d, the SEM analysis of microstructural changes are analyzed for surfaces irradiated with 1520 nm fs-pulse lasers over 30 s, 120 s, and 300 s, respectively. As explained above, since the laser focal spot was fixed during short period of mineral irradiation which meant that at the focus all the incident energy was concentrated over a small area. In contrast with the CW laser experiments on pellets, discussed above in Figures 5a to 5d, the irradiation with the 1520 nm fs-pulse laser for

periods between 30 s and 300 s exhibited better interaction with mineral, resulting in a more uniform densification and occlusion of dentinal tubules in and around the laser irradiated area, as exemplified in Figures 6b to 6d. The scale of structural modification extends 3 to 5 times beyond the dimension of focal spot (250 μm), and is in sharp contrast with the melting and crystallization type of features in Figures 5c and 5d.

The fixed focussing of laser at one point during irradiation leads to high energy density, which is the ratio of average power (130 mW) divided by the beam focal area (250 $\mu m^2$), producing a crater-like feature by displacing the materials sideways via a wave-assisted displacement, as is observed during a classical semi-plastic/plastic material flow. The typical behaviour of materials flow under laser irradiation was verified by repeating the irradiation experiments with pressed mineral pellets and human molars, in order to analyze a large cross-sectional area between the natural and the synthetic enamel minerals, and then comparing the data with that for human molar. Figure 7a is a cross-sectional image before fs-laser sintering which can be distinguished from the microstructure after sintering, as shown in Figures 7b and 7c.

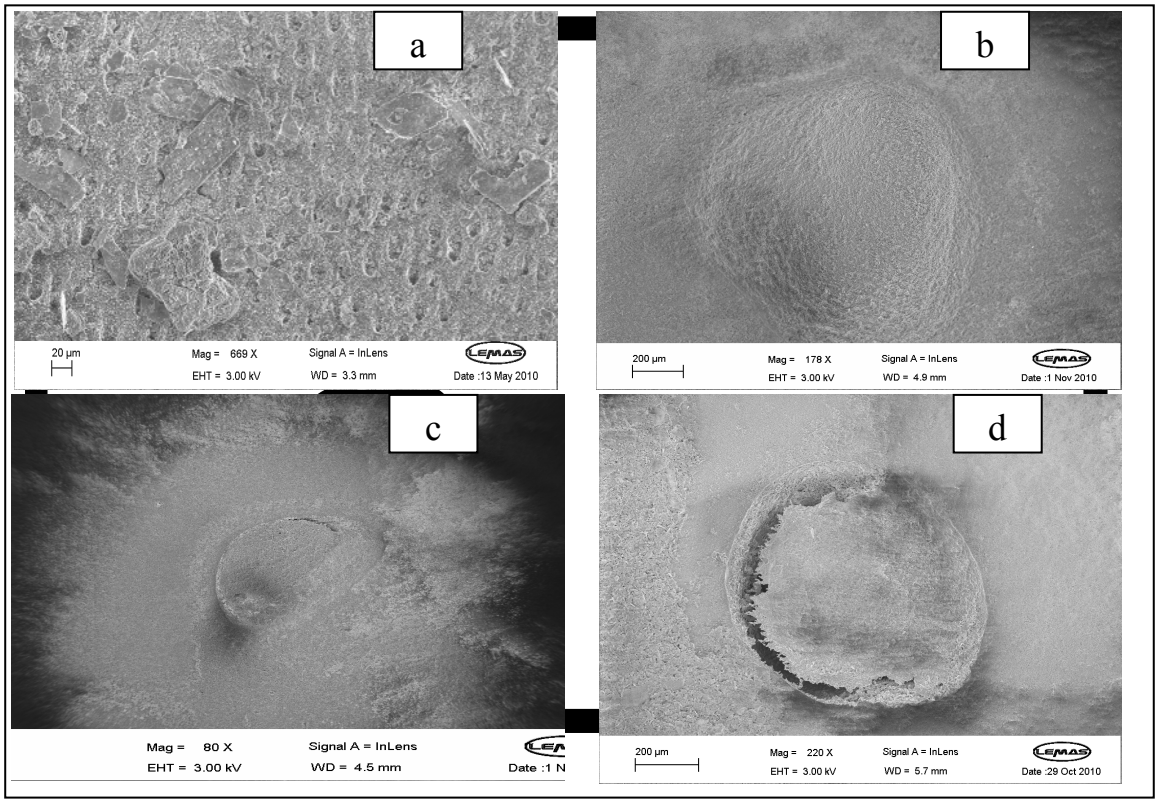


**Figure 6. SEM images of a tooth section coated with CaP composite irradiated with 1520 nm pulse laser for (a) before irradiation microstructure, showing platelets of doped CaP minerals; (b) 30 seconds; and (c) 120 seconds; and (d) 300 seconds of irradiation. The fixed focussed spot of laser induces damage due to large energy density.**

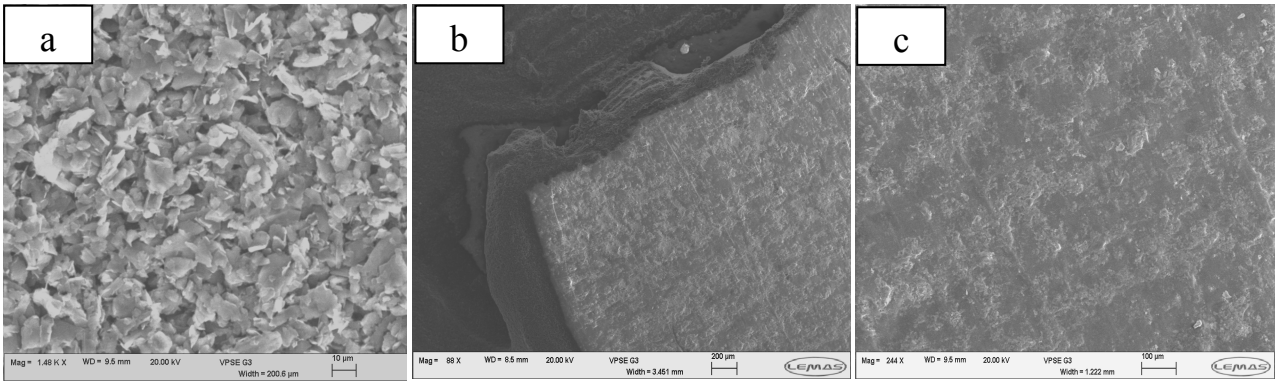


**Figure 7. Comparison of densification of a doped CaP pressed pellet with fs-laser (1520 nm) irradiation. (a) shows the porous structure before fs-laser sintering; (b) after 15 seconds of irradiation, and (c) is a high magnification image of area in (b) showing evidence for particle densification on a microscopic scale.**

The superficial melting is apparent from the microstructure in Figure 7c which is at 10x lower magnification than the micrograph of unsintered pellet in Figure 7a. In Figure 7b around the light grey regions of sintered pellet we also observe a ridge of finer materials which was deposited via the acoustic vibration generated during fs-laser irradiation.

Figure 8 shows the cross-sectional microstructure of dentine with a 1520 nm fs-laser-sintered overlayer of doped mineral which has formed after 60 seconds of irradiation, yielding roughly 50 μm thickness over the dentine.

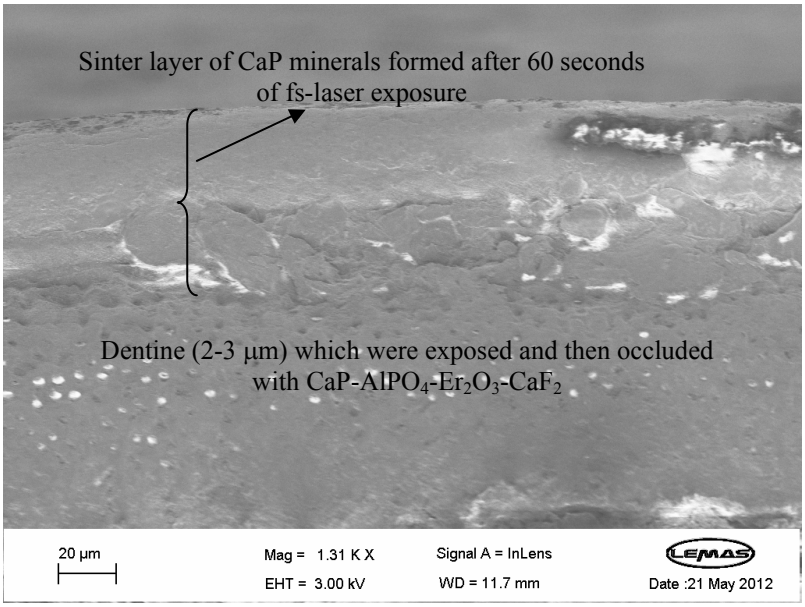


**Figure 8. An SEM image of the cross-section of molar, showing dentine tubules which are occluded with a 50 μm thick layer of doped CaP mineral, containing $Er_2O_3$, $AlPO_4$, and $CaF_2$.**

The preliminary measurements of micro-hardness of the occluded surface was performed after 5 minutes of irradiation using a 980 nm source, as shown in Figure 5d where we had observed

localized melting and formation of rosette-like crystals. The measured hardness of melted and solidified mineral over occluded dentine was 1100 MPa, when compared with data for exposed dentine surface which was 240 MPa. The increase in hardness with respect to exposed dentine surface confirms the restoration of enamel by occlusion. Detailed material structure and adhesion characterisation for CW and fs-laser are under investigation and will be reported in future.

## 4. Conclusion

The present study reports the results of a research methodology for the treatment of tooth sensitivity by analyzing the microstructures of post laser-mineral interaction. In this study on enamel mineral resurfacing using lasers, the photo-active $Er^{3+}$-doped calcium phosphate mineral phase was mixed with $AlPO_4$ and $CaF_2$. It was observed that using a 980 nm CW laser power (150 mW) the $CaF_2$ containing mineral melted and solidified over a period of 5 minutes of irradiation. The effect of melting was less apparent when a 1520 nm CW laser was used. By contrast, the effect of irradiation using a 120 fs-pulsed laser at 1520 nm has a dramatic effect on mineral densification, which was achieved within 60 seconds. The densified laser, as shown in Figure 8, appears to be 50 μm thick.

## Acknowledgements

The authors of this paper acknowledge the financial support from the RCUK funded Basic Technology (EP/D048672/01) and EPSRC/TSB supported Integrated Knowledge Centre projects, which were essential for generating the data.

## Conflict of Interest

The authors declare there is no conflict and interest.

## References

1. Bender IB (2000) Pulpal Pain Diagnosis-A Review. *J Endod* 26: 1-5.
2. Addy M (2002) Dentin hypersensitivity: new perspectives on an old problem *Int Dent J* 52: 367-375.
3. Walters PA (2005) Dentinal hypersensitivity: A Review. *J Contemp Dent Pract* 6(2): 107-117.
4. Schafer F, Beasley T, Abraham P (2009) In vivo delivery of fluoride and calcium from toothpaste containing 2% hydroxyapatite. *International Dental J* 59(6): 321-324.
5. Aranha AC, Pimenta LA, Marchi GM (2009) Clinical evaluation of desensitizing treatments for cervical dentin hypersensitivity. *Braz Oral Res* 23 (3): 333-339.
6. Earl JS, Milne SJ, Wood D (2008) In Vitro Study of dentin tubule infiltration by hydroxyapatite and Silica Nanoparticles. 1-16.
7. Roveri N, Battistella E, Bianchi CL, et al. (2009) Surface Enamel Remineralization: Biomimetic Apatite Nanocrystals and Fluoride Ions Different Effects. *J Nanomaterials* 1-9.
8. Bigi A, Boanini E, Capuccini C, et al. (2007) Strontium-substituted hydroxyapatite nanocrystals. *Inorg Chim Acta* 360 (3): 1009-1016.
9. Matthew M, Takagi S (2001) Structures of Biological Minerals in Dental Research. *J Res Natl Inst Stand Technol* 106 (6): 1035-1044.
10. Byrappa K, Yoshimura M (2001) Handbook of hydrothermal technology 7-14, 287-295.
11. Resende NS, Nele M, Salim VMM (2006) Effects of anion substitution on the acid properties of hydroxyapatite. *Thermochim Acta* 451(1-2): 16-21.

12. Mayer I, Layani JD, Givan A, et al. (1999) La ions in precipitated hydroxyapatites. *J Inorg Biochem* 73(22): 1-6.
13. Boanini E, Gazzano M, Bigi A (2011) Ionic substitutions in calcium phosphates synthesized at low temperature. *Acta Biomaterialia* 6: 1882-1894.
14. Bartl MH, Scott H, Wirnsberger G, et al. (2002) Synthesis and luminescence properties of mesostructured thin films activated by in-situ formed trivalent rare earth ion complexes. *Chem Commun* 21: 2474-2475.
15. Zhang C, Matsumoto K, Kimura Y, et al. (2006) Effects of $CO_2$ laser in treatment of cervical dentinal hypersensitivity. 24 (9): 595-597.
16. Husein (2006) An Applications of Lasers in Dentistry: A Review. *Arch Orofac Sci* 1: 1-4.
17. Elmadani E, Jha A, Peralli T, et al. (2012) Characterization of Rare-Earth Oxide Photoactivated Calcium Phosphate Minerals for Resurfacing Teeth. *J Am Ceram Soc* 1-7.
18. Shellis RP, Heywood BR, Wahab FK (1997) Formation of Brushite, Monetite and Whitelocktite During Euilibration of Human Enamel with Acid Solutions at 37°C. *Caries Res* 31:71-77.
19. Fernandez TT (2010) Femtosecond laser written optical waveguide amplifier in phospho-tellurite glass. *Optics Express* 18(19): 20289-20297.
20. Jha A, Richards B, Jose G, et al. (2012) Rare-earth ion doped $TeO_2$ and $GeO_2$ glasses as laser materials. *Prog Mater Sci* 57(8): 146-149.